RSC Advances

PAPER

View Article Online
View Journal | View Issue

Cite this: *RSC Adv.*, 2026, **16**, 1163

Thermal stability and flame retardancy of cellulose nanocrystals reinforced epoxy nanocomposites

Hoor Albarqi,[ac] Mohamad Nurul Azman Mohammad Taib, *[b] Tawfik A. Saleh[cd] and Viswanathan S. Saji [c]

Epoxy is a type of thermosetting resin that has been widely used in different applications, such as for adhesives, sealants, coatings, paneling, and electronics boards, due to its excellent mechanical strength and chemical resistance. Despite its advantages in mechanical performance, epoxy has drawbacks related to flammability and compromised thermal stability. This drawback has a profound impact on the final processing and applications of epoxy resin. In this study, a bio-based additive, cellulose nanocrystal (CNC), was successfully developed and added to the epoxy resin to enhance the flame retardancy and thermal performance of the resulting epoxy composite. CNC was extracted from cotton linters and used directly as an additive to the epoxy matrix, with varying concentrations (0.5 wt% and 1.0 wt%). The fabricated epoxy composites were evaluated for flammability using a cone calorimetry test and for thermal stability by thermogravimetric analysis. The thermal stability results obtained were significant; 0.5 wt% and 1.0 wt% CNC-added epoxy composites demonstrated a significant improvement in the onset of thermal degradation. The cone calorimetry test revealed a 17% reduction in peak heat release rate (pHRR) and total heat release rate (HRR), indicating substantial improvements in flame resistance. The CNC promoted the char formation in the epoxy matrix due to the absence of oxygen in the char layer, thus preventing further flame penetration into the inner layer. The CNC-reinforced epoxy has the potential to be used as a flame-retardant additive in polymer composite applications as well as in coating parts where heat and thermal resistance are important.

Received 9th November 2025
Accepted 20th December 2025

DOI: 10.1039/d5ra08642f

rsc.li/rsc-advances

1. Introduction

Epoxy resin is a thermosetting polymer that is frequently used as a matrix in the production of composite materials, including nanocomposites.[1] Epoxy has advantages such as high durability and mechanical performance, chemical resistance, good compatibility, and superior bonding with organic and inorganic substances.[2] Despite the benefits of this resin, certain downsides, such as limited petrochemical resources, flammability, low thermal stability, environmental unfriendliness, and production costs, limit its application.[3] Epoxy is compatible with various nanoscale materials, including nanosilica, carbon nanomaterials, and nanoclays, among others, to overcome the drawbacks of epoxy. Researchers have tried to develop more sustainable and eco-friendly epoxy composites with added biomass and bio-based materials such as cellulose.[4,5]

Flame retardants (FRs) have become an intriguing choice for use in polymeric materials. FR agents are applied to reduce the propagation of fire, preventing it from entering or completely burning the materials. It has become vital for polymers to be fire-resistant since FR agent can provide improved qualities when employed in harsh and flammable circumstances. The polymers, including epoxy, have a tendency to burn and melt, releasing a large amount of poisonous smoke.[6] This is because polymers, including epoxy, naturally tend to melt when exposed to heat or fire, which means they have the potential to be toxic to water, humans, and animals. Traditional FRs that are added to polymers typically contain halogenated compounds, which can leak and damage landfills and water sources and produce hazardous smoke that can impair respiratory function.[7] Due to this reason and to lower emissions and carbon footprint, the bio-derived cellulose-based FRs have high significance. An appropriate addition of FRs could slow the ignition of flames, build up a protective char layer, or lessen the rate at which fire spreads.[8] Table 1 shows the pros and cons of conventional and biopolymer-based flame retardants (FRs). Cellulose is among the bio-based materials that have been discovered to be more environmentally friendly and abundantly available, with cellulose acting as a flame-retardant additive.

[a]*King Abdulaziz and His Companions Foundation for Giftedness and Creativity "Mawhiba", Riyadh, Saudi Arabia*

[b]*Institute for Advanced Studies (IAS), University of Malaya, 50603 Kuala Lumpur, Malaysia. E-mail: azman_88@um.edu.my*

[c]*Interdisciplinary Research Center for Advanced Materials, King Fahd University of Petroleum & Minerals, Dhahran, 31261, Saudi Arabia*

[d]*Chemistry Department, King Fahd University of Petroleum & Minerals, Dhahran, 31261, Saudi Arabia*

Table 1 The pros and cons of conventional and biopolymer-based flame retardants (FRs)[9–11]

Biopolymers FRs		Conventional FRs	
Positive	Negative	Positive	Negative
Does not contain any harmful compounds when burned or heated	Suitable for short-term periods of use, possibility of degradation	Good for lengthy-term periods of application	Produce hazardous chemicals while burning or heating, causing health concerns, and are not eco-friendly
Biodegradable	Easy to leach and decompose in soil, disposable	Non-biodegradable and may remain for a long period	Contaminants are easily leached and can remain in the soil for a long time, contaminating food, soil, and landfills
Comparable to conventional- FRs in terms of flame retardancy, mechanical, and other performances	Several preparation steps include the usage of solvents/chemicals	Improve mechanical, physical, and flame-retardant properties, among others	Extraction requires a lot of energy, and there are several process steps
Low cost and requires little energy for production, but excellent char production to produce FR protective layer	Poor compatibility and dispersion with polymer matrices	Expensive and involves higher production costs	Poor sustainability and negative impact on material properties (causing plasticization, brittleness, or color changes)

Table 2 An analysis of reported works on cellulose nanocrystal (CNC) source, extraction method, matrix of composite, and properties investigated

Cellulose type	Source	Method of extraction	Matrix of composite	Properties investigated	Ref.
CNC	Kenaf	H_2SO_4 hydrolysis and ultrasonic treatment	Poly(vinyl alcohol)	Morphology, structure, and thermal properties	17
CNC	Cotton	H_3PO_4 hydrolysis	Ethylene oxide–epichlorohydrin copolymer	Morphology, structure, crystallinity, thermal stability, mechanical properties	20
CNC	*Posidonia oceanica*	H_2SO_4 hydrolysis	Poly(styrene-*co*-butyl acrylate)	Morphology, thermal properties, and dynamic mechanical analysis	21
CNC	Tunicin whiskers	H_2SO_4 hydrolysis	Poly(oxyethylene)	Morphology, structure, thermal and dynamic mechanical analysis	22
CNC	Cotton	H_2SO_4 hydrolysis	Polyoxyethylene and low-density polyethylene	Viscoelastic, morphology, and thermal properties	23
CNC	Microcrystalline cellulose	H_2SO_4 hydrolysis	Poly(3-hydroxybutyrate-*co*-3-hydroxyvalerate)	Morphology, structure, thermal, and dynamic mechanical properties	24
CNC	Oil palm frond	H_2SO_4 hydrolysis	Alginate hydrogel	Morphology, structure, BET, adsorption isotherm modelling	25
CNC	Cottonseed linter	H_2SO_4 hydrolysis	Foam nitrile rubber	Crosslinking density, morphology, structure, dynamic mechanical behavior	26
CNC	Cornhusk	H_2SO_4 hydrolysis	—	Structural, morphology and thermal properties, particle size and zeta potential analysis	27
CNC	Cellulose	Not stated	Nitrile butadiene rubber latex	Mechanical properties, crosslink density, and resistance to high-pressure hydrogen exposure	28
CNC	Cottonseed linter	H_2SO_4 hydrolysis	Nitrile rubber	Morphology, thermal and mechanical properties	29
CNF	Not stated (purchased from University of Maine-Process Development Center, USA)	Not stated	Polyurethane	Chemical, thermal, mechanical, morphological and limiting oxygen index	30
CNF	Cellulose microcrystalline	Mechanical grinding	Bio-epoxy	Morphology, structure, and mechanical properties	31
CNC	Cellulose microcrystalline	Hydrolysis with tannic acid	Polyamide 66	Flame retardancy, antibacterial and UV resistance	32

Cellulose is a type of polysaccharide composed of glucose monomer units and is the most abundant natural biopolymer, with around 40–90% extracted from plants or biomass, depending on the sources. Cotton is considered to be 90% built up of cellulose.[12] Another well-known source for cellulose is kenaf (*Hibiscus cannabinus*), which has been planted commercially as a commodity crop in countries such as Malaysia, China, India, and Brazil.[13] In general, the cellulose sources can be classified as woody and non-woody plant-based materials.[14] Table 2 details the different sources and extraction methods of CNCs along with their matrices and investigated properties. The cellulose chains are primarily made from amorphous and crystalline regions. The amorphous region can be removed entirely and broken down to form nano-sized cellulose, also known as cellulose nanocrystalline or cellulose nanofibrils (CNF).[15] Depending on the synthesis method, the CNC is obtained from hydrolysis mostly by using strong acid hydrolysis. Whereas CNF is extracted using mechanical methods such as through a homogenizer or grinding. The CNC has a high crystallinity region that contributes to overall performance, including mechanical properties, thermal stability, and flame retardancy.[16,17] CNC can be used as an additive to epoxy composites to reduce the dependency on epoxy polymer and overcome the limitations, such as low thermal stability and flame resistance.[18] This characteristic also favors agglomeration when added to a polymer matrix, so it is necessary to control the additive and limit its addition to a small percentage to create a uniform and stable dispersion.[19]

The goal of this study is reducing flammability and improved thermal stability of epoxy composites with addition of CNC as additive. Typical reported studies utilized nano-sized cellulose in different polymer matrices and mainly focused on their mechanical properties (Table 2). Only a few studies among them have focused on the thermal stability and flame retardancy of composites for use in various high-end applications. In this study, we investigate the thermal stability and flammability of CNC as an additive in epoxy composite. We extracted the CNC from cotton linter cellulose. Then, the CNC was added to epoxy to form epoxy nanocomposites with different CNC concentrations (0.5 wt% and 1.0 wt%). The developed nanocomposites were thoroughly characterized using TEM, XRD, FTIR, and EDX. The flammability test was performed using cone calorimetry, and the thermal stability was analyzed using thermogravimetric analysis (TGA). SEM and FTIR were used to study the samples before and after cone calorimetry tests. The results indicate that the CNC–epoxy composite developed in this study can be used for final applications such as fire-retardant coatings and composites.

2. Experimental

2.1 Materials

Cotton linter with an average length of 12 mm and a diameter of 20 μm was bought from a local supplier. All chemicals, including hydrochloric acid, were AR grade. Bisphenol A (epichlorohydrin) as the epoxy and *N*-(3-dimethylaminopropyl)-1,3-propylene diamine as the hardener were used to fabricate the epoxy composite and nano epoxy composites. Epoxy and hardener, purchased from Sigma-Aldrich, were used without further purification.

2.2 Cellulose nanocrystal (CNC) preparation by acid hydrolysis

5 g of cotton linter cellulose was placed in a round-bottom flask, which was surrounded by an ice bath within a 1 L beaker. HCl acid was incrementally added, drop by drop, until a concentration of 5 M was attained. The ice bath was thereafter removed, and the bottom flask was heated until it reached 100 °C and maintained for 60 minutes with continuous stirring at 500 rpm. Upon completion of the hydrolysis procedure, the mixture was immediately quenched with ice cubes to halt the reaction, followed by multiple rinses with distilled water and centrifugation to eliminate the unreacted acid. The mixture was subsequently filtered, placed in a dialysis tube, and immersed in deionized (DI) water until it attained a pH of 7. The final suspension was dried using a freeze dryer prior to its application in subsequent operations. The quantity of CNC acquired was 2 g. The experimental parameters were selected based on the preliminary experiments by Taib *et al.*[33]

2.3 Composite fabrication

The epoxy composites were prepared using the solution casting method. Initially, the CNC at concentrations of 0, 0.5 wt%, and 1.0 wt% was combined with epoxy and hardener with a ratio of 3 to 1 in a beaker through stirring. The solution was subsequently poured into a silicon mold measuring $100 \times 100 \times 30$ mm^3 and allowed to cure overnight for around 24 hours at room temperature. The samples were labeled as neat epoxy, 0.5 wt% CNC/epoxy, and 1.0 wt% CNC/epoxy, respectively.

2.4 Characterization

2.4.1 Transmission electron microscopy (TEM). Firstly, 0.1 wt% of the CNC sample was added in deionized (DI) water. The solution was subjected to ultrasonication for 30 min to avoid particle agglomeration. Using a plastic dropper, one drop for each sample was placed onto a copper grid. After that, the sample was allowed to dry at room temperature for 60 s. Filter paper was used to get rid of the excess solution. A TEM microscope (Zeiss Libra 120, Carl Zeiss NTS GmBH) with an accelerating voltage of 120 kV was used.

2.4.2 Fourier transform infrared spectroscopy (FTIR). FTIR equipped with an ATR accessory was used to determine the functional groups of the neat epoxy and its composites. Analysis was carried out from 4000 cm^{-1} to 600 cm^{-1} with 16 scans using a PerkinElmer FTIR instrument.

2.4.3 X-ray diffraction (XRD). X-ray diffraction patterns were recorded on a PANalytical X'Pert PRO MPD diffraction system for the CNC sample in order to examine the changes in crystallinity of the material. The device operated at 40 kV and 35 mA current, with monochromatic Cu Kα ($\lambda = 1.54$ Å). The Segal equation (eqn (1)) was used to calculate the crystallinity index (CrI).[34] The analysis and peak determination were carried out using PANalytical HighScore Plus 3.0d software.

$$\mathrm{CrI} = \frac{I_{200} - I_{\mathrm{am}}}{I_{200}} \times 100\% \quad (1)$$

whereas I_{200} is the intensity of the principal peak (200) lattice diffraction (at I_{200}, $2\theta = 22.5°$ for cellulose I).[35] For I_{am} that refers to the intensity of diffraction for amorphous cellulose (at $2\theta = 18°$ for cellulose I).[36]

2.4.4 Thermogravimetry analysis (TGA). The thermal stability of neat epoxy and its composites was investigated using thermogravimetry analysis, TGA Q-500 (TA Instruments, USA). Approximately 10 mg of each sample was weighed in a pan and operated under a continuous flux of nitrogen gas (50 mL min^{-1}). All the samples were heated from room temperature to 900 °C, with a 10 °C min^{-1} ramp.

2.4.5 Flame retardancy. The flame retardant evaluation on epoxy and its composites was conducted using the cone calorimeter model GD-ISO5660B-M by following the procedures of ISO 5660 under a heat flux of 50 kW m^{-2} with the sample size of 100 × 100 × 30 mm^3.

2.4.6 Scanning electron microscopy (SEM). The microstructures and morphologies of CNC and their composites were observed by using a scanning electron microscopy (SEM) instrument (SU3500, Hitachi, Tokyo, Japan). The samples were sputter-coated with a thin layer of gold to avoid charges. Accelerating voltage at 20 kV in low vacuum was used to avoid samples burning.

2.4.7 Energy dispersive X-ray analysis (EDX). The EDX analysis was conducted on CNC. Initially, the sample was weighed, approximately 0.05 g, and then placed on a double tab that was conductive with carbon. Following this, the samples underwent a gold sputter coating to reduce charging effects and distortion. The images were acquired using a scanning electron microscope fitted with an Oxford Instruments X-max 50 mm^2 dispersive X-ray detector, functioning at an accelerating voltage of 5 kV in a high vacuum environment.

3. Results and discussions

3.1 Transmission electron microscopy (TEM)

Fig. 1 presents the TEM micrographs of the prepared CNC. The CNC exhibited platelet-like and spherical shapes, with agglomeration observed among the CNC particles. The CNC has been verified to exhibit nanoscale widths and microscale lengths. The TEM analysis revealed that the CNC had a length of 178.12 ± 74.18 nm and a width of 91.22 ± 35.58 nm, resulting in an aspect ratio of 12.06 ± 0.65. The significant variations in the standard deviation of length and width are due to inconsistency in getting the same size of CNC, as evident from Fig. 1. The present result is in line with the author's previous work,[17] where CNC with a length around 283 ± 84.35 nm and a width of 38.93 ± 13.31 nm was extracted from kenaf.

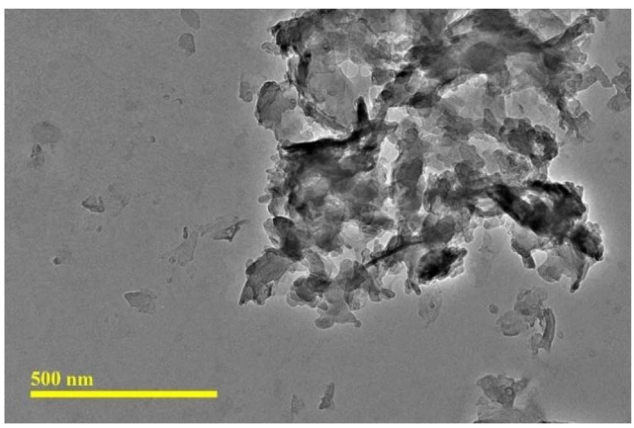

Fig. 1 TEM images of prepared cellulose nanocrystals (CNC).

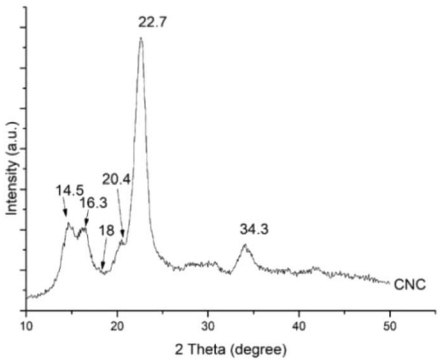

Fig. 2 XRD diffraction spectra of cellulose nanocrystals (CNC).

3.2 X-ray diffraction (XRD)

The XRD pattern in Fig. 2 shows a typical cellulose I structure.[35] The crystallinity of CNC may result in a decreased reinforcing capability within polymer composites.[37] The crystalline structure of CNC significantly influences its reinforcing effects and ensures that it maintains this property when incorporated and reinforced within a polymer matrix. Fig. 2 illustrates the observed diffraction peaks at 2θ angles of approximately 14.5, 16.3, 20.4, 22.7, and 34.3, which correspond to the reflection planes of cellulose I, namely [1−10], [110], [012], [200], and [004], respectively.[36] The findings demonstrated that the crystalline structure remained intact, exhibiting the typical cellulose configuration, with a recorded crystallinity index of 84.79%, calculated using the Segal equation as outlined in eqn (1).

3.3 Energy dispersive X-ray spectroscopy (EDX)

The EDX spectrum of the CNC is shown in Fig. 4. The main components of CNC are carbon (C) and oxygen (O). The

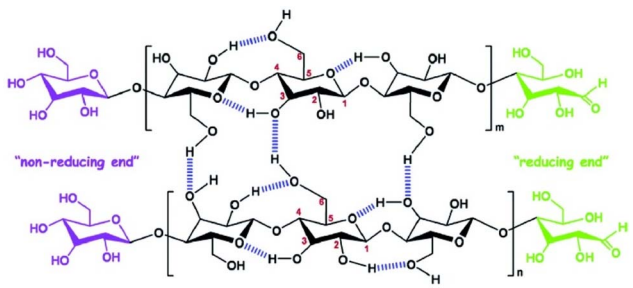

Fig. 3 Schematic diagram of cellulose nanocrystal structure for anhydroglucose unit on the backbone of the cellulose for three reactive hydroxyl groups (positions C2, C3 and C6).

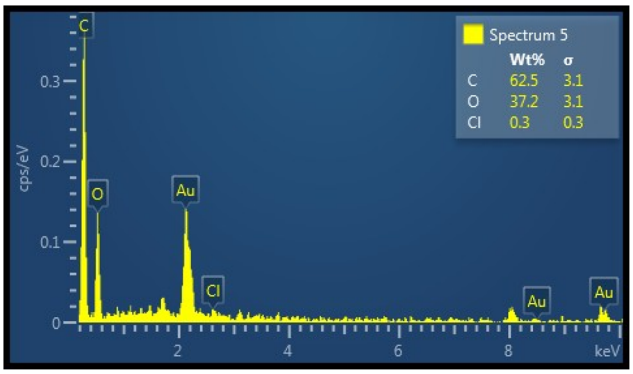

Fig. 4 EDX spectra and elemental identification of cellulose nanocrystals (CNC). The Au signal corresponds to Au sputtering used for sample preparation.

percentage compositions of C, O, and Cl were 62.5 wt%, 37.2 wt%, and 0.3 wt%, respectively. The chemical structure of CNC (Fig. 3) evidences the existence of C and N and the slight trace of Cl, which can be contributed by HCl during hydrolysis and that left over after repeated washing.

3.4 Thermogravimetric analysis (TGA)

The thermal stability and decomposition of neat epoxy and its composites were assessed through TGA analysis. The information is summarized in Table 3, and the TGA and DTG thermograms are presented in Fig. 5(a) and (b). In Fig. 5(a), two distinct peaks were observed for the decomposition of neat epoxy and its composites. The area below 150 °C can be associated with the elimination of present water and volatile organic compounds.[38] In the temperature range of 300 °C to 500 °C, the degradation peaks of the composites exhibited overlap, with the onset temperature for neat epoxy recorded at 291 °C, while the 0.5 wt% CNC/epoxy and 1.0 wt% CNC/epoxy showed onset temperatures at 303 °C and 313 °C, respectively. The presence of CNC exhibiting a high crystallinity index may explain the elevated onset degradation observed in the epoxy composites, as high energy adsorption is required in order to allow for disarrangement prior to further degradation. Another contributing factor can be the increased cross-linking density of epoxy resin after compositing.[39] This in line with the study conducted by Taib *et al.*,[40] using nitrile butadiene polymer also exhibited a high onset degradation after CNC was added into the polymer. In Fig. 5(b), the maximum degradation temperature (T_{max}) of neat epoxy was found to be 373 °C; however, upon the incorporation of CNC, the T_{max} increased to 376 °C and 381 °C for the 0.5 wt% CNC/epoxy and 1.0 wt% CNC/epoxy, respectively. The

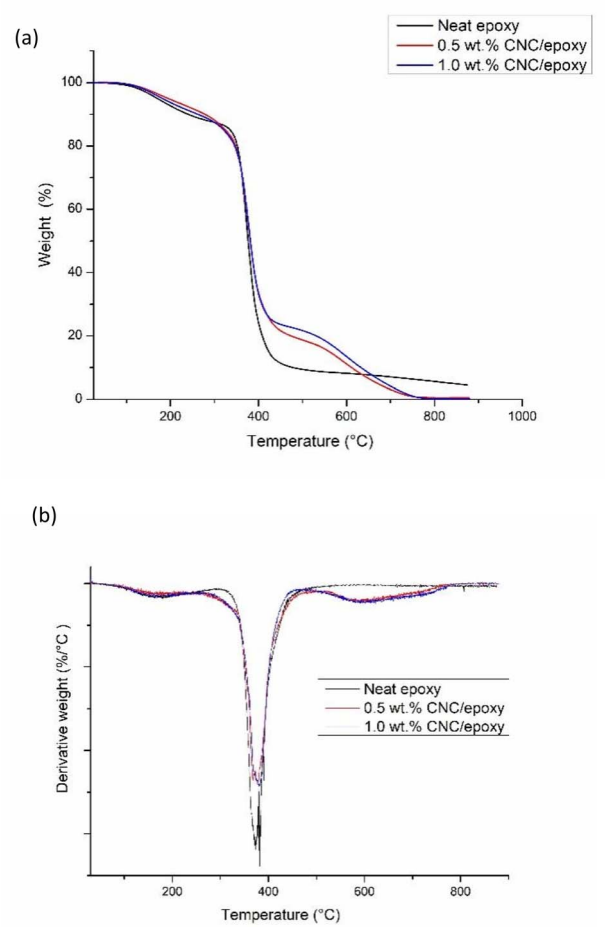

Fig. 5 (a) TGA; (b) DTG for neat epoxy, 0.5% CNC/epoxy and 1% CNC/epoxy.

increase of T_{max} could be related to complex degradation pathways of CNC in an epoxy matrix.[17] The maximum mass loss rate (MLR_{max}) for 0.5 wt% CNC/epoxy was decreased with a value of 1.18 wt% min^{-1} compared to neat epoxy (1.51 wt% min^{-1}) and for 1.0 wt% CNC/epoxy which was 1.20 wt% min^{-1} due to the formation of porous structures following the thermal degradation of CNC can lead to a reduction in thermal conductivity, but this would be benefited by incorporating an additive filler that would enhance the property.[41] Therefore, the addition of 0.5 wt% CNC into the epoxy composite was enough to effectively form a char layer for protection against heat. This was in line with a study conducted by Gan *et al.*[42] with the addition of halogen-free additive within waterborne polyurethane (WPU). The MLR_{max} value was

Table 3 Data obtained from TGA thermogram

Type of samples	Onset degradation temperature, T_0 (°C)	Maximum decomposition temperature, T_{max}[a] (°C)
Neat epoxy	291	373
0.5 wt% CNC/epoxy	303	376
1.0 wt% CNC/epoxy	313	381

[a] Derived from DTG curve.

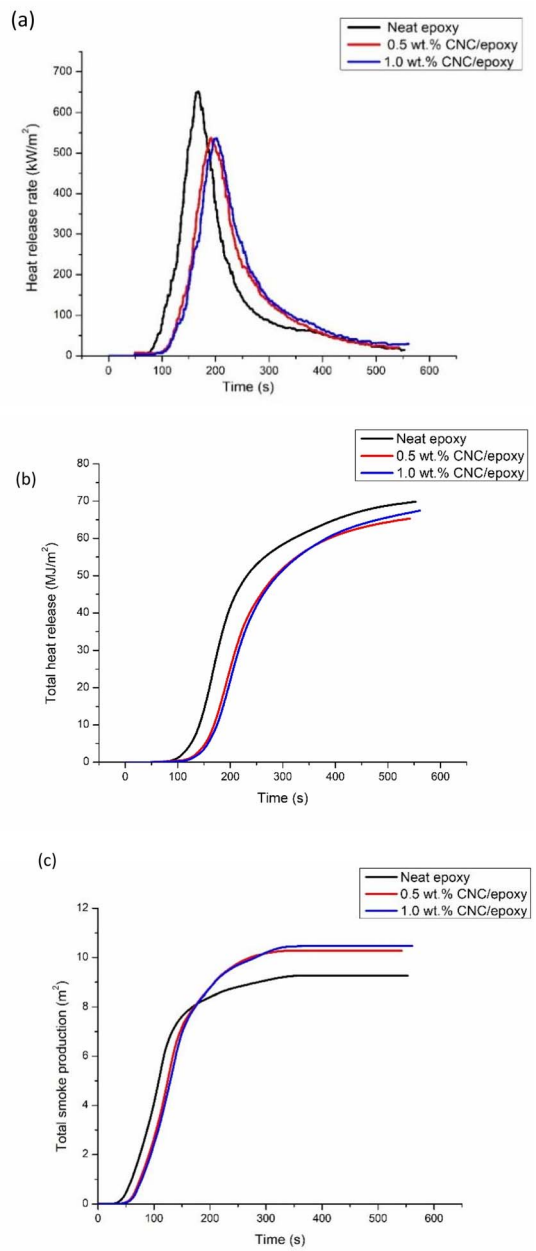

Fig. 6 The properties after cone calorimeter test (a) heat release rate (HRR), (b) total heat release (THR) and (c) total smoke production (TSP) of neat epoxy, 0.5 wt% CNC/epoxy and 1.0 wt% CNC/epoxy.

decreased after the addition of this filler and suggested the formation effective char protection and the suppressing mass loss at high temperatures. Different studies were conducted by Zhou *et al.*[43] and Zhang *et al.*[44] that suggested it was worth noting that with the increase of functional additives in polymer, the maximum mass loss rate (MLR_{max}) would gradually increase with the second decomposition peak merged with the first decomposition peak, which makes the decomposition faster and earlier. The final degradation phase for CNC was at 400 °C. This was in line with a previous study conducted by Taib *et al.*[2] with CNC from oil palm trunk reinforced in epoxy composite.

Table 4 Cone calorimeter data of epoxy and epoxy composites[a]

Sample	TTI (s)	pHRR (kW m^{-2})	THR (MJ m^{-2})	TSP (m^2)
Epoxy	13	651.61	69.16	9.2
0.5 wt% CNC/epoxy	17	537.56	63.98	10.3
1.0 wt% CNC/epoxy	20	537.02	67.09	10.5

[a] TTI = time to ignition, pHRR = peak heat release rate, THR = total heat release, TSP = total smoke production.

This temperature was associated with the degradation of the remaining epoxy components.

3.5 Flame retardancy

Cone calorimeter tests represent a highly effective method for assessing the flammability of composites in conditions that simulate real burning scenarios. Fig. 6(a)–(c) show the plots corresponding to the heat release rate (HRR), total heat release (THR), and total smoke production (TSP) for the neat epoxy and its composites, with the key details listed in Table 4. The time to ignition, or TTI, plays a crucial role in assessing the delay before a fire begins to burn a sample. The highest value for TTI was recorded for 1.0 wt% CNC/epoxy composite within 20 s, followed by 0.5 wt% CNC/epoxy (17 s) and neat epoxy (13 s). In Fig. 6(a), the highest peak heat release rate (pHRR) was recorded for neat epoxy, which shows a poor flame resistance. With the addition of 0.5 wt% and 1.0 wt% of CNC within epoxy, the pHRR values were reduced to 537.56 kW m^{-2} and 537.02 kW m^{-2}, respectively, compared with the neat epoxy that was 651.61 kW m^{-2}. This variation suggests that the addition of 0.5 wt% of CNC into epoxy was enough to reduce the flammability of epoxy from continuing to propagate. The similar trend was observed in Fig. 6(b) for total heat release (THR). There was possible filler saturation/agglomeration as the CNC was hydrophilic that contributed to this result. This reduction was around 17% for 1.0 wt% CNC/epoxy composite as compared to neat epoxy. This suggested better flame resistance. Fig. 6(c) for total smoke production (TSP) values indicate that minimal smoke was released for neat epoxy during the combustion process. The addition of CNC leads to an increase in smoke production due to the formation of the char layer that prevented the flame from penetrating. The TSP value obtained for 0.5 wt% CNC–epoxy composite was 10.3 m^2 and that for 1.0 wt% CNC–epoxy was 10.5 m^2, both were higher than that of neat epoxy, which was 9.2 m^2. This variation suggests that the production of smoke suppressed the fire from further burning. The comparison of the present results with other analogous reports are stated in Table 5. The 0.5 wt% CNC/epoxy and 1.0 wt% CNC/epoxy produced the lowest pHRR compared to other additives in Table 4. The THR was among the lowest and it was only a little bit higher compared to the nanoclays/epoxy (1.0 wt%, 3.0 wt% and 5.0 wt%).[45] Hence, the present results confirm that the addition of 0.5 wt% CNC in epoxy is enough to give good improvement

Table 5 Comparison of flame retardant and thermal properties of reported epoxy composites[a]

Composite type	TTI (s)	PHRR (kW m^{-2})	THR (MJ m^{-2})	TSP (m^2)	Char residue (%)	T_{on} (°C)	T_{max} (°C)	Ref.
Nanoclays/epoxy 1 wt%	—	558	26.42	8.88	—	—	—	47
Nanoclays/epoxy 3 wt%	—	570	25.48	10.01	—	—	—	
Nanoclays/epoxy 5 wt%	—	533	24.83	8.18	—	—	—	
1 wt% graphene-ox/epoxy	49	1204	81	27	12.9	357	415	45
3 wt% graphene-ox/epoxy	47	1244	72	25	14.1	359	418	
1 wt% graphene-Cu/epoxy	45	825	66	24	8.1	334	411	
3 wt% graphene-Cu/epoxy	47	786	64	23	11.0	343	409	
0.8 wt% SiO_2/epoxy	53.3	1138.9	103.9	—	—	339.2	—	48
1.5 wt% SiO_2/epoxy	52.7	1141.9	97.0	—	—	338.6	—	
2.3 wt% SiO_2/epoxy	52.7	1022.4	90.2	—	—	338.5	—	
3.9 wt% SiO_2/epoxy	54.7	910.9	84.4	—	—	343.2	—	

[a] Graphene OX; graphene oxide; graphene-Cu; graphene doped copper; SiO_2: nano silica; TTI = time to ignition; PHRR = peak heat release rate; THR = total heat release; TSP = total smoke production rate; T_{on} = onset degradation temperature; T_{max} = maximum degradation temperature.

for pHRR and HRR. The main enhancement mechanism is CNC promoting the formation of a char layer in the epoxy surface, thus hindering the heat and flame from the char areas and blocking oxygen gases. This prevented the inner layer of epoxy from further burning, thus the integrity of the structure of the epoxy was not totally compromised. The addition of FR would promote the char formation and hinder the penetration of flame to the inner part of the material.[46]

3.6 Morphology of char residues using scanning electron microscopy (SEM)

Fig. 7(a)–(f) display the SEM surface morphology of neat epoxy, 0.5 wt% CNC–epoxy, and 1.0 wt% CNC–epoxy samples, both before and after the cone calorimetry tests. For 0.5 wt% and 1.0 wt% of CNC reinforced epoxy, the fiber and matrix have good adhesion and no porosity, with some agglomeration occurring. However, some cracks, voids, and fissures were observed for all the samples after the cone calorimetry test. The 0.5 wt% (Fig. 7(d)) and 1.0 wt% CNC/epoxy (Fig. 7(f)) samples show a continuous and denser char layer with some cracks observed at ×10 000 magnification. The denser char layer forms a protective insulator against flame. The oxygen gas in this area is less, and the flame could not penetrate the char layer. The addition of 0.5 wt% and 1.0 wt% CNC to epoxy enhances the char residue formation, which protects the epoxy matrix and results in lower heat release. This is in agreement with a study by Wang *et al.*[49] on epoxy nanocomposites, where the added nano additives in the form of carbon nanotubes enhanced the char formation, which protected the inner layer of polymer from further combustion.

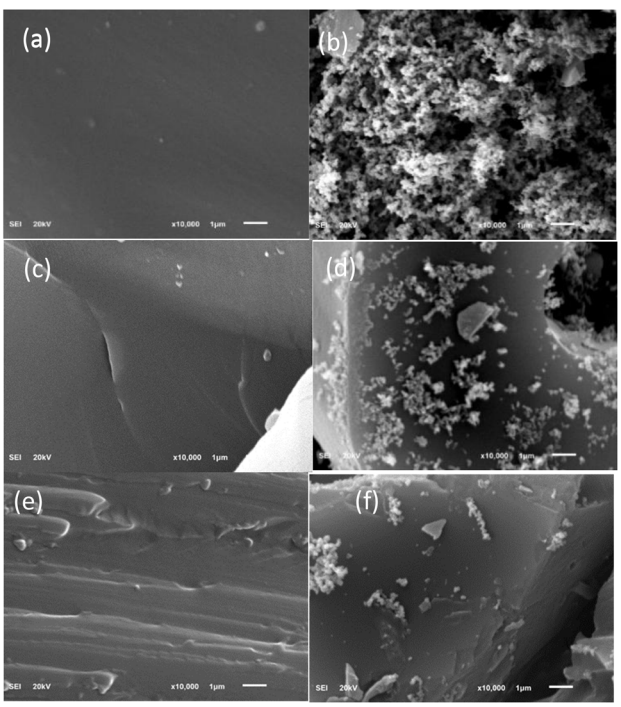

Fig. 7 Surface morphology of samples (a, c and e) before and (b, d and f) after cone calorimetry studies: (a and b) epoxy; (c and d) 0.5 wt% CNC/epoxy and (e and f) 1.0 wt% CNC/epoxy.

3.7 Fourier transform infrared (FTIR)

Fourier transform Infrared spectroscopic analysis was used to identify the interaction of the epoxy and the curing agent on CNC before and after the cone calorimetry tests. Fig. 8 displays the FTIR spectra for epoxy control, 0.5 wt% CNC/epoxy, and 1.0 wt% CNC/epoxy before and after cone calorimeter tests. In Fig. 8(a) for epoxy control, it showed the typical broad peak around 3500–3000 cm^{-1}, which is attributed to –OH stretching vibration of the OH groups.[50] The OH peak disappeared after the cone calorimeter test for epoxy control and composites due to dehydration. The OH reduction after 0.5 wt% CNC and 1.0 wt% CNC was due to OH interaction between particles and matrix. The peaks corresponding to -C-H group was observed around 2800–2900 cm^{-1}.[51] Whereas those corresponding to CH_2 was appeared at 2324 cm^{-1} and 2361 cm^{-1} (Fig. 8). Both peaks were seen to increase after the addition of CNC due to overlapped peaks as well as the result of increased crosslinking of CNC in the epoxy polymer chains. These peaks were reduced after the cone calorimeter test due to the degradation process. The C=O peak was observed at 1730 cm^{-1}. This peak can be correlated with the appearance of ester carbonyl group.[52] The

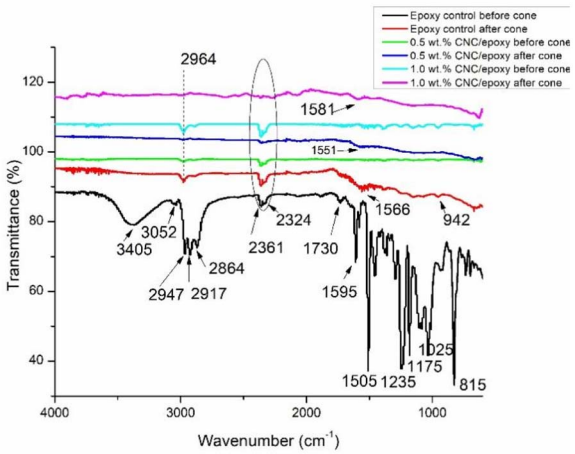

Fig. 8 FTIR spectra of epoxy and CNC/epoxy composites before and after cone calorimetry test.

amine groups for the hardener used in epoxy composites had appeared at 1595 cm^{-1} and 1505 cm^{-1}, respectively. These peaks were attributed to the –NH bend found in primary amides and the amide linkages attributed to the presence of C═O.[53] The peak at 2964 cm^{-1} appeared at 0.5 wt% CNC/epoxy and 1.0 wt% CNC/epoxy, corresponding to C–H group in cellulose and organic matter. This peak was reduced after the cone calorimeter test due to the degradation process. In Fig. 8(a) The formation of carbon compound was observed with the existence of peaks at 1550 to 1600 cm^{-1} and at peak 942 cm^{-1} after the cone calorimetry test.[54] The SEM and FTIR results support that degradation occurred with the formation of carbon-based materials (char residues) after the test was conducted.

4. Conclusions

In a nutshell, this study evaluated the effect on thermal stability and flame retardancy following the incorporation of a low loading additive of cellulose nanocrystals (CNC) in epoxy composites. The CNC exhibits a cellulose I crystal structure, characterized by a crystallinity index of 84.79%. The compositing resulted in the integration of high crystallinity CNC into epoxy, showcasing a notable degree of intramolecular hydrogen bonding and distinct crystal structure properties. The incorporation of CNC at low loading levels examined in this study (up to 1.0 wt%) facilitated improved dispersion, resulting in a well-dispersed homogeneous mixture within the polymer matrix with little agglomeration. CNCs with a lower aspect ratio used in this work improved the nucleation phenomenon throughout the crystallization process. The thermal stability of epoxy reinforced with CNC is significantly altered after the addition of 1.0 wt% CNC, attributed to the crystalline structure of CNC and the enhancement of crosslinking density within the polymer matrix. The addition of CNC resulted in enhanced flame retardancy, with 1.0 wt% CNC addition would yield a better property enhancement in epoxy, promoting a char layer that served as an effective barrier. The results were further validated by SEM and FTIR analyses. This study, hence, successfully produced CNC as additive in epoxy composites with good thermal and flame-retardant properties when compared to the neat epoxy. The agglomeration tendency of CNC in the epoxy needs to be further studied, and these findings contribute to the effectiveness of the FR additive. Surface modification of the CNC to improve its compatibility and distribution in the epoxy matrix needs to be explored. Additionally, there is a need for further research on the application of these composites in various fields, including electrical and electronic, chemical resistance, environmental effects, and industrial utilization, where wide applications of this composite can be utilized.

Author contributions

H. Albarqi: investigation, writing – original draft. M. N. A. M. Taib: writing – original draft, writing – review and editing, supervision. T. A. Salleh: writing – review and editing. V. S. Saji: writing – review and editing.

Conflicts of interest

There are no conflicts to declare.

Data availability

Data will be made available upon request.

Acknowledgements

This research is supported by Universiti Malaya Research Excellence Grant 2025 (UMREG002-2025). The authors would like to thank to Universiti Malaya for technical supports. Special thanks to King Abdul Aziz Model Schools for sponsorship of Mawhiba program for Ms H. Albarqi and King Fahd University of Petroleum & Minerals for provided a place for Mawhiba study.

References

1 H. Sukanto, W. W. Raharjo, D. Ariawan, J. Triyono and M. Kaavesina, *Open Eng.*, 2021, **11**, 797–814.
2 M. N. A. M. Taib, *RSC Adv.*, 2025, **15**, 45061–45070.
3 S. Sasidharan and A. Anand, *Ind. Eng. Chem. Res.*, 2020, **59**, 12617–12631.
4 C. Santulli, in *Eco-Friendly Adhesives for Wood and Natural Fiber Composites: Characterization, Fabrication and Applications*, Springer, 2021, pp. 131–145.
5 T. Aziz, H. Fan, X. Zhang, F. U. Khan, S. Fahad and A. Ullah, *J. Polym. Eng.*, 2020, **40**, 314–320.
6 P. M. Doley, A. C. Y. Yuen, I. Kabir, L. Liu, C. Wang, T. B. Y. Chen and G. H. Yeoh, *Fire*, 2022, **5**, 139.
7 B. L. Chean-Yiing, S. Y. Yusuf, N. R. Jamian, R. M. Kasmani, A. M. Rashid, D. Naidu, E. A. Wikurendra and A. H. Z. Fasya, *Biointerface Res. Appl. Chem.*, 2022, **12**, 7983–7993.
8 M. M. S. Mohd Sabee, Z. Itam, S. Beddu, N. M. Zahari, N. L. Mohd Kamal, D. Mohamad, N. A. Zulkepli,

M. D. Shafiq and Z. A. Abdul Hamid, *Polymers*, 2022, **14**, 2911.
9 Z. Kovačević, S. Flinčec Grgac and S. Bischof, *Polymers*, 2021, **13**, 741.
10 M. Maqsood and G. Seide, *Biomolecules*, 2020, **10**, 1038.
11 X. Wang, E. N. Kalali, J.-T. Wan and D.-Y. Wang, *Prog. Polym. Sci.*, 2017, **69**, 22–46.
12 R. S. Dassanayake and N. Abidi, *Cotton Fibres*, 2017, 207.
13 I. B. Kamal, *J. Sci. Technol.*, 2014, **6**, 41–66.
14 J. Pennells, I. D. Godwin, N. Amiralian and D. J. Martin, *Cellulose*, 2020, **27**, 575–593.
15 D. Trache, M. H. Hussin, M. M. Haafiz and V. K. Thakur, *Nanoscale*, 2017, **9**, 1763–1786.
16 M. N. A. M. Taib, T. S. Hamidon, Z. N. Garba, D. Trache, H. Uyama and M. H. Hussin, *Polymer*, 2022, **244**, 124677.
17 M. N. A. M. Taib, T. S. Yee, D. Trache and M. Hazwan Hussin, *Cellulose*, 2024, **31**, 997–1015.
18 Y. Yang, W. Chen, Z. Li, G. Huang and G. Wu, *Chem. Eng. J.*, 2022, **450**, 138424.
19 M. A. H. Howlader, *Preparation, functionalization and derivation of nanocrystalline cellulose*, 2015.
20 S. Camarero Espinosa, T. Kuhnt, E. J. Foster and C. Weder, *Biomacromolecules*, 2013, **14**, 1223–1230.
21 F. Bettaieb, R. Khiari, A. Dufresne, M. F. Mhenni and M. N. Belgacem, *Carbohydr. Polym.*, 2015, **123**, 99–104.
22 M. A. S. A. Samir, F. Alloin, J.-Y. Sanchez and A. Dufresne, *Polymer*, 2004, **45**, 4149–4157.
23 K. Ben Azouz, E. C. Ramires, W. Van den Fonteyne, N. El Kissi and A. Dufresne, *ACS Macro Lett.*, 2012, **1**, 236–240.
24 E. Ten, J. Turtle, D. Bahr, L. Jiang and M. Wolcott, *Polymer*, 2010, **51**, 2652–2660.
25 T. S. Hamidon, N. N. Idris, R. Adnan, M. M. Haafiz, A. Zahari and M. H. Hussin, *Int. J. Biol. Macromol.*, 2024, **262**, 130239.
26 Y. Chen, Y. Zhang, C. Xu and X. Cao, *Carbohydr. Polym.*, 2015, **130**, 149–154.
27 X. Yang, F. Han, C. Xu, S. Jiang, L. Huang, L. Liu and Z. Xia, *Ind. Crops Prod.*, 2017, **109**, 241–247.
28 S. Ye, S. Yasin, H. Zhi, Y. Song, C. Gu and J. Shi, *Fibers*, 2025, **13**, 29.
29 X. Cao, C. Xu, Y. Wang, Y. Liu, Y. Liu and Y. Chen, *Polym. Test.*, 2013, **32**, 819–826.
30 H. Kim, J. Park, K. S. Minn, J. R. Youn and Y. S. Song, *Macromol. Res.*, 2020, **28**, 165–171.
31 P.-Y. Kuo, L. de Assis Barros, N. Yan, M. Sain, Y. Qing and Y. Wu, *Carbohydr. Polym.*, 2017, **177**, 249–257.
32 X. Ma, Y. Zhang, H.-Y. Yu, B. Jia, X. Wang, X. Chen and X. Yang, *Int. J. Biol. Macromol.*, 2024, **283**, 137994.
33 M. Taib, W. A. Yehye and N. M. Julkapli, *Cellul. Chem. Technol.*, 2020, **54**, 11–25.
34 L. Segal, J. J. Creely, A. Martin Jr and C. Conrad, *Text. Res. J.*, 1959, **29**, 786–794.
35 K. S. Salem, N. K. Kasera, M. A. Rahman, H. Jameel, Y. Habibi, S. J. Eichhorn, A. D. French, L. Pal and L. A. Lucia, *Chem. Soc. Rev.*, 2023, **52**, 6417–6446.
36 M.-C. Stanciu, F. Tanasă and C.-A. Teacă, *Polysaccharides*, 2025, **6**, 30.
37 S. Kumar, G. Graninger, S. C. Hawkins and B. G. Falzon, *Composites, Part A*, 2021, **148**, 106475.
38 J. A. Conti Silva, H. Walton, S. Dever, K. Kardel, T. Martins Lacerda and R. Lopes Quirino, *Coatings*, 2022, **13**, 25.
39 S. Kumar, L. Prasad, P. P. Bijlwan and A. Yadav, *Biomass Convers. Biorefin.*, 2024, **14**, 12673–12698.
40 M. N. A. M. Taib, W. A. Yehye, N. M. Julkapli and S. B. O. A. Hamid, *Fibers Polym.*, 2018, **19**, 383–392.
41 M. Antlauf and O. Andersson, *Macromolecules*, 2022, **55**, 5326–5331.
42 J. Gan, J. Zhou, Y. Xu, T. Zhang and X. Zhang, *ACS Appl. Polym. Mater.*, 2024, **6**, 9974–9985.
43 J. Zhou, T. Zhang, Y. Xu and X. Zhang, *Prog. Org. Coat.*, 2023, **182**, 107631.
44 T. Zhang, Y. Xu, J. Dai and X. Zhang, *Prog. Org. Coat.*, 2025, **205**, 109315.
45 Y. Liu, H. V. Babu, J. Zhao, A. Goñi-Urtiaga, R. Sainz, R. Ferritto, M. Pita and D.-Y. Wang, *Composites, Part B*, 2016, **89**, 108–116.
46 Z. Sun, Y. Hou, Y. Hu and W. Hu, *Mater. Chem. Phys.*, 2018, **214**, 154–164.
47 T. Ngo, Q. Nguyen, T. Nguyen and P. Tran, *Arabian J. Sci. Eng.*, 2016, **41**, 1251–1261.
48 M. Häublein, K. Peter, G. Bakis, R. Mäkimieni, V. Altstädt and M. Möller, *Materials*, 2019, **12**, 1528.
49 Q. Wang, X. Pan, C. Lin, D. Lin, Y. Ni, L. Chen, L. Huang, S. Cao and X. Ma, *Chem. Eng. J.*, 2019, **370**, 1039–1047.
50 M. G. González, J. C. Cabanelas and J. Baselga, *Infrared Spectroscopy-Materials Science, Engineering and Technology*, 2012, vol. 2, pp. 261–284.
51 J. Liu, K. Chen, Y. Zhang, L. Zhou, F. Wang, X. Xiang and H. Wu, *Prog. Org. Coat.*, 2024, **196**, 108677.
52 Z. Heng, Y. Chen, H. Zou and M. Liang, in *Handbook of Epoxy Blends*, Springer, 2017, pp. 147–184.
53 M. Khajouei, P. Pouresmaeel-Selakjani and M. Latifi, *Bio-Based Epoxy Polymers, Blends and Composites: Synthesis, Properties, Characterization and Applications*, 2021, pp. 267–281.
54 A. A. Kareem and H. K. Rasheed, *Mater. Sci.*, 2019, **37**, 622–627.